

A Connectivity Strategy for the Evaluation of Smart Grid Models Based on the Ethernet Technology

A. I. Narvaez-Villota , *Member, IEEE*, A. J. Ustariz-Farfan , *Member, IEEE*, and
L. F. Diaz-Cadavid , *Member, IEEE*

Abstract—A simulation strategy that enables data transmission between the modeled components of a Smart Grid is proposed in this paper. The proposed simulation strategy, referred to as the connectivity strategy, enables the integration of a physical communication network into Smart Grids simulations. The connectivity strategy comprises three steps: selection of Smart Grids functionality, data transmission over a TCP/IP network, and connectivity strategy evaluation. Each step is described to ensure transparency and reproducibility in Smart Grid simulations, addressing the limitations associated with the lack of specifications when a communication network is implemented into power systems simulations. Furthermore, a Hardware-in-the-loop (HIL) approach is presented for developing and evaluating the proposed connectivity strategy using the HIL technique. Through this approach, the strategy is validated by establishing the communication between simulation and embedded systems via a physical Ethernet network. In a case study, the use of the connectivity strategy to simulate a distribution system automation (DA) functionality is demonstrated. This simulation allows the evaluation of protection schemes in a Smart Grid using MATLAB/Simulink and a Texas Instruments development kit. Results show that the proposed connectivity strategy could estimate the communication delays for different simulation scenarios.

Link to graphical and video abstracts, and to code: <https://latamt.ieeer9.org/index.php/transactions/article/view/8657>

Index Terms—Distributed Generation, Embedded Systems, Ethernet, Hardware-in-the-loop, Lightweight TCP/IP Stack, Smart Grid.

I. INTRODUCTION

Smart Grids offer a range of benefits, including flattening out peak demand, improving power quality and reliability, and reducing greenhouse emissions [1]. To achieve these benefits, Smart Grids facilitate the integration of modern communication and information technologies into traditional power systems [2]. These modern technologies allow power systems to have new functionalities, such as Advanced Metering Infrastructure (AMI), Distribution System Automation (DA), and Distributed Energy Resources (DER) support, among others [3]–[5].

A Smart Grid introduces new operational scenarios compared to traditional power systems, influenced by

communication networks. Consequently, the behavior of Smart Grid components responsible for monitoring, protection, and control operations can be significantly affected by data transmission and their interactions with other components. Recognizing this, traditional simulation tools may not adequately model the behavior of these new power systems. Hence, the development of simulation strategies to evaluate Smart Grid component models and their interactions is necessary [6], [7].

Previous research works have addressed this challenge through the implementation of Smart Grid models employing different simulation strategies. These strategies include building Smart Grid models within a single simulation tool [8]–[10], utilizing co-simulation [11]–[13], and HIL (Hardware-in-the-Loop) techniques [14]–[17]. However, some limitations have been identified. Models implemented within a single simulation tool may lack the inclusion of communication networks or power system specifications. Additionally, there is a tendency observed in the implementation of communication networks as black boxes.

To fill the gap, this paper proposes a simulation strategy—the connectivity strategy, to allow data transmission between different Smart Grids components through a physical Ethernet communication network. The connectivity strategy has a series of structured steps. It provides detailed specifications for the communication network, which can be integrated into the simulations of power systems. By applying the proposed connectivity strategy, delays associated with integrating a communication network into Smart Grid models can be identified. Such delays reflect the real-world situation where the communication network takes time to transfer the measured data and control signals.

This paper is a substantially expanded follow-up of the previous research work of the authors [18]. In the previous work, an electrical power system was built in MATLAB/Simulink® in one computer, and a protection scheme controller was simulated in another computer. An earlier version of the connectivity strategy was used for the communication between the controller and the power system models between the two computers. In addition to the previous research work, in this paper, the protection scheme controller was modeled in a Texas Instruments® development kit while the power system was simulated in MATLAB/Simulink®. The newly proposed connectivity strategy enables communication between the embedded system and the simulation software.

In this paper, a case study of a Smart Grid was implemented based on the modified IEEE 34-bus distribution system. The

This work was supported by the Universidad Nacional de Colombia, Manizales Campus.

A. I. Narvaez-Villota, A. J. Ustariz-Farfan, and L. F. Diaz-Cadavid are with the Universidad Nacional de Colombia, Manizales, Caldas, Colombia (e-mails: ainarvaezv@unal.edu.co, ajustarizf@unal.edu.co, and lfidiazc@unal.edu.co).

proposed connectivity strategy was adopted in the Smart Grid model to evaluate an adaptive protection scheme. The real-time communication between the Smart Grid components was realized through a physical Ethernet network. Further, a HIL approach, which includes hardware components in the simulation environment, was employed to evaluate the effectiveness of the proposed connectivity strategy.

The rest of the paper is organized as follows: section II describes the proposed connectivity strategy. Section III discusses the application of the proposed strategy. Section IV shows the case study. Finally, we conclude the paper and propose future work in section V.

II. CONNECTIVITY STRATEGY PROPOSAL

This section presents the proposed simulation methodology—the connectivity strategy. This strategy allows the simulation of Smart Grids models to include a physical communication network. The connectivity strategy has three steps: selection of Smart Grids functionality, data transmission over a TCP/IP network, and connectivity strategy evaluation.

A. Step 1: selection of Smart Grids functionality

In this paper, the DA functionality in Smart Grids is chosen for its impact on enhancing service continuity and quality [4], [19]. This Smart Grid functionality requires components for monitoring, control, and protection operations, which are typically facilitated through Intelligent Electronic Devices (IEDs) [20]. Additionally, a Local Control Center (LCC) is selected to make decisions based on the data provided by these IEDs

1) Monitoring IED

The monitoring IED calculates the RMS current of the three-phase power systems using the method proposed by Buchholz [21]:

$$I_{RMS_3F} = \sqrt{\frac{1}{T_0} \int_{T_0} [i_a^2(t) + i_b^2(t) + i_c^2(t)] dt}, \quad (1)$$

where I_{RMS_3F} is the RMS current of the three-phase power system; $i_a(t)$, $i_b(t)$, and $i_c(t)$ are the currents of each conductor; and T_0 is the period.

2) Protection IED

This Smart Grid component is modeled as a digital relay that has different protection functions and it has been developed by the Power Quality and Power Electronics Research Group (GICEP) and the Transmission and Distribution Network Research Group (GREdYP) [22]. In this paper, the 50/51 overcurrent inverse time and instantaneous protection function with communication was selected. Its settings can be updated based on data received from other components in the electrical power system.

For the overcurrent protection, or 51, the tripping time $t(I)$, in seconds is based on the IEEE C37.112-1996 standard [23] and calculated in equation (2).

$$t(I) = \frac{A}{\left(\frac{I_{en}}{I_p}\right)^P - 1} + B, \quad (2)$$

where I_{en} is the current at the connection point with the distribution line; I_p is the pickup current; A , B , and P are the constants defined according to the tripping time curve used. A multiplier t_{esc} can be used for the new trip time with delay: $t(I) * t_{esc}$.

For the instantaneous protection function, or 50, the trip time is directly given as an input: t_{ins} ; and ESC_{ins} , which corresponds to the scale of the adjustment current in terms of I_p .

The output of the IED device is the binary tripping signal. When the fault duration exceeds $t(I)$ or t_{ins} , a value of 0 is given and the switch is opened. Otherwise, the value is 1 and the switch remains closed.

3) Local Control Center

A local control center (LCC) makes the decisions in the distribution system of a Smart Grid through its interaction with the IEDs. The LCC can dynamically update the setup parameters of the protection IEDs when the topology of the Smart Grid changes, as proposed by the authors in [24]–[28].

The specific LCC algorithm used in the case study for this paper will be further discussed in subsequent sections.

B. Step 2: Data Transmission over a TCP/IP Network

The Smart Grid model has components for monitoring, control, and protection operations. Those components are deployed in different end devices and should be able to communicate among themselves. The communication architecture for data transmission among the end devices is described in this section. Ethernet is selected for the testing in this paper as it is one of the most common ways of communication. Ethernet is compatible with the protocols of the TCP/IP model.

1) Algorithms for Data Reception and Transmission

An interface is required to make the interconnection between the Smart Grid model and the actual communication infrastructure. The flow chart of the algorithm for sending and receiving data is shown in Fig. 1. The Smart Grid components, deployed in different end devices, can send or receive data through the interfaces. When any Smart Grid component requires sending or receiving data, the simulation will be interrupted, awaiting the completion of data transmission, with a default timeout of up to 1 second. This interruption is proposed for single-threaded power systems simulations.

2) Communication Architecture

Two different end devices communicate via the communication infrastructure over a physical Ethernet network. The communication infrastructure has multiple layers, and each of them uses protocols based on the TCP/IP model, as described below [29].

a) Application Layer

The client-server model is used for the application layer. The application layer uses an Application Programming

Interface (API), which provides the interface between the Smart Grids model and the transport layer. Data can be transmitted in ASCII code format.

b) Transport Layer

The Transmission Control Protocol (TCP) is a connection-oriented protocol that has reliability in the transmission and reception of data. In this paper, TCP is used in full-duplex mode, facilitating bidirectional data transmission for Smart Grid components reliant on received or transmitted data.

c) Network Layer

The Internet Protocol (IP) is used for the network layer. The assignment of the IP addresses in each end device can be done statically or dynamically. The dynamic IP address assignment requires the use of the Dynamic Host Configuration Protocol (DHCP) [30].

d) Data Link and Physical Layer

The Fast Ethernet technology complying with the IEEE 802.3u 100Base-T standard has been chosen [31]. This technology has compatibility with most of the hardware components that communicate through Ethernet.

3) Network Configuration

The use of a local area network (LAN) is proposed to allow real-time data transmission among different end devices. The proposed network shown in Fig. 2, utilizes a star topology, which is a common configuration for LANs, however, the connectivity strategy is adaptable to other network topologies.

In this configuration, different end devices can be connected through a layer 2 Ethernet switch and an IP router that belongs to layer 3.

Additionally, in this proposal, the IP addresses of the end devices are dynamically assigned by enabling the DHCP server functionality of the IP router. This simplifies the process of connecting end devices to the network.

C. Step 3: connectivity strategy evaluation

The communication process is illustrated in Fig. 3. The data transmission between the applications from different end devices is evaluated by the communication delay, which is measured according to the IEEE 1646-2004 standard [32]. In this paper, the applications are the simulated components of the Smart Grid model. Additionally, the communication delay has been modified to include the processing time of the algorithm of one of the applications. This communication delay t_{com} is defined in equation (3).

$$t_{com} = t_1^1 + t_2^1 + 2t_3 + t_1^2 + t_2^2 + t_4, \quad (3)$$

where t_1^1 and t_1^2 are the time to extract the data from the application and to write these data to the interface; t_3 is the time over the communication network; t_2^1 and t_2^2 are the time to read the data from the interface and then upload them to the application; t_4 is the time to execute the algorithm in application 2. The communication delay is measured on the end device 1.

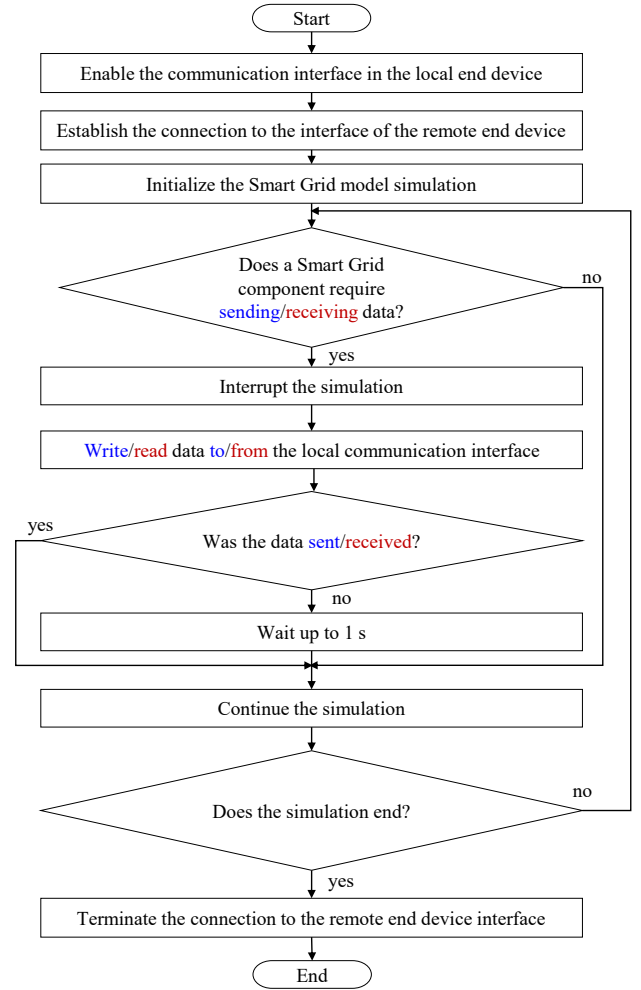


Fig. 1. Flowchart of the algorithm for sending (in blue) or receiving data (in red).

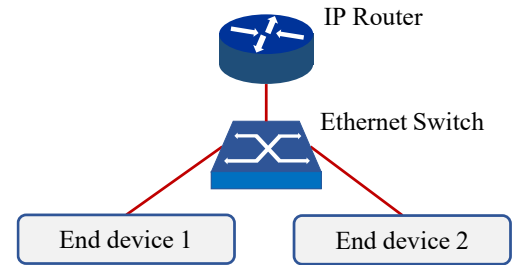


Fig. 2. LAN with a star topology. End devices connect to a layer 3 IP Router via a layer 2 Ethernet switch.

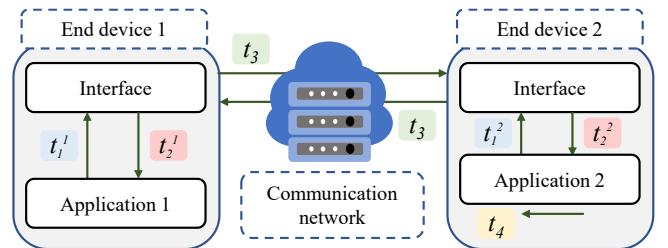


Fig. 3. Application-to-application communication delay.

III. HIL APPROACH

This section describes the development and evaluation of the proposed connectivity strategy based on the HIL technique.

A. Development of the HIL Approach

A Smart Grid model was created with its monitoring IED and protection IED in MATLAB/Simulink® and the LCC in the Hercules™ RM57Lx Launchpad™ development kit from Texas Instruments® [33]. The proposed connectivity strategy enables communication between the different components in the Smart Grid model.

A Smart Grid library with the components for the monitoring IED, the protection IED, and the LCC was created and used in the proposed connectivity strategy. The components for the monitoring IED and the protection IED were created in MATLAB/Simulink® as Simulink® blocks. The LCC was created in the development kit as a function in the C programming language.

The proposed connectivity strategy also includes a server-client network application. For the simulation in MATLAB®, the interface between the Simulink® blocks and the transport layer is established using the TCP sockets, which are provided by the MATLAB® Instrument Control Toolbox™ in the TCP/IP objects [34]. In the development kit, the interface between the C function and the transport layer is established using the RAW API, which is available in the LWIP library [35], [36]. The recommended configurations and the integration of LWIP [37] are taken as a basis for this study.

The MATLAB® simulation provides the client socket, while the development kit runs the RAW API as the server. After establishing the connection between the client and the server, the monitoring IED and the protection IED in MATLAB® simulation and the LCC in the development kit could exchange data through the process shown in the block diagram (Fig. 4).

In the computer, the transmitter-receiver block realizes the two functions: “Acquisition/Load data” and “Write/Read in the client socket”. This block is based on the algorithm shown in Fig. 1. This block enables the transmission of data between the communication network and the blocks of the library in Simulink®.

In the development kit, the receiver-transmitter function realizes two functions: “Read/Write in the server RAW API” and “Load/Acquire data”. This function is created in C Language and based on the algorithm shown in Fig. 1. The receiver-transmitter function is responsible for the transmission of data between the communication network and the selected function from the Smart Grid library.

B. Performance Evaluation

A test scenario has been implemented to evaluate the performance of the HIL approach, in which the computer and the development kit exchange messages, as shown in Fig. 5.

During each test, a message A is sent from end device 1 to end device 2. Sequentially, end device 2 sends a message B in response. These messages involved in the data exchange are

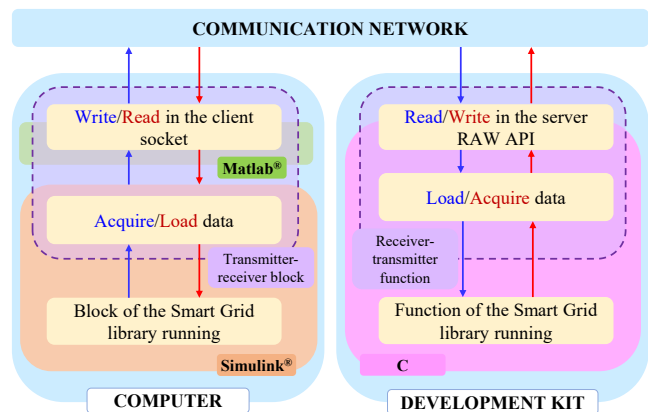


Fig. 4. Process for the transmission and reception of data between the components of the Smart Grid. The transmitter-receiver block was created in MATLAB® to allow data exchange between the communication network and the Simulink® environment. The transmitter-receiver function was created in C language to allow data exchange between the communication network and the embedded system.

the payload for the TCP segments. Each message is an array containing 8-bit unsigned integer data (uint8).

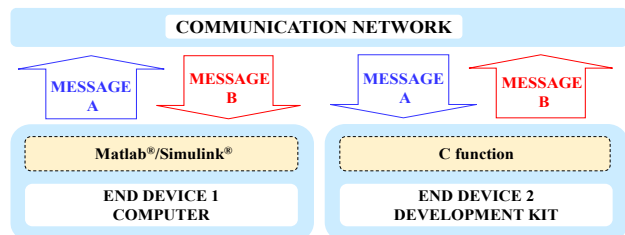


Fig. 5. Diagram of the data exchange process for the test scenario.

The scenario has five tests, in which the size of message A remains constant, while the size of message B changes for each test. In addition, the communication delay is measured during the tests. The sizes of the two messages, the average communication delay (AVG t_{com}), the standard deviation (σ), and the 95% confidence interval (CI) obtained for each test with 10000 executions, are shown in Table I.

It can be seen that communication delays between 11.98 and 59.89 ms were obtained in real-time. The communication delay gradually increased as the size of message B increased, due to the longer processing time for the read/write operations on interfaces and data files.

TABLE I
COMMUNICATION DELAY VARIATION BASED ON THE MESSAGE SIZES

Test	Message A size [Bytes]	Message B size [Bytes]	AVG t_{com} [ms]	σ [ms]	CI [ms]
1	6	190	11.98	5.24	[10.96, 13.01]
2	6	256	15.84	2.18	[15.41, 16.27]
3	6	512	17.93	2.18	[17.50, 18.35]
4	6	1024	22.79	3.20	[22.16, 23.42]
5	6	2048	59.89	4.95	[58.92, 60.86]

IV. CASE STUDY

The modified IEEE 34-bus distribution system is used for the case study of a Smart Grid with two topologies: the DG

topology, which has the power source from both the main grid and distributed generation, and the radial topology, which is connected only to the main grid. The modeling and parameters used in the Smart Grid are from previous research [22], [38], [39]. When the monitoring IEDs detect the changes in the topology from the Smart Grid, the LCC will make decisions to update the parameter settings of the protection IEDs. During the process, all the data transmission will be enabled by the proposed connectivity strategy in HIL. The case study evaluates the real impacts of the communication delay.

The Smart Grid has three sources, as presented in the single-line diagram (Fig. 6): the electrical main grid (EG), the distributed generator 1 (G1), and the distributed generator 2 (G2). Each source has a monitoring IED: M-P800, M-P848, and M-P890 respectively. The Smart Grid has five protection IEDs: RL1, RL2, RL3, RL4, and RL5. In the case study, a fault occurs on bus 846.

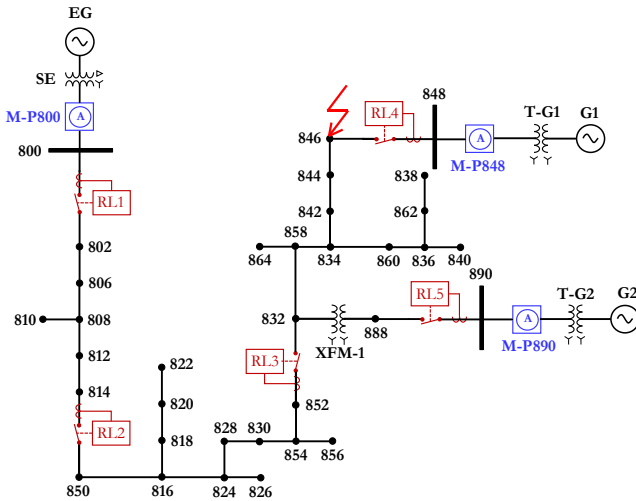


Fig. 6. Single-line diagram of the modified IEEE 34-bus distribution system.

The parameters of the sources and transformers are presented in Table II and Table III, respectively. The protection IEDs settings are defined in Table IV for each operation topology of the IEEE 34-bus system [22]. The protection coordination for the DG topology is defined in Group 1, where both EG, G1, and G2 are in operation. The protection coordination for the radial topology is defined in Group 2, where only EG is in operation. The constants A , B , and P , for protection function 51 are defined by the IEC Standard Inverse Time curve.

TABLE II
SOURCES PARAMETERS

Source	Line voltage [kV]	f [Hz]	3-phase short circuit level [MVA]	X/R ratio
EG	69	60	100	7
G1	0.48	60	100	1
G2	0.48	60	100	1

TABLE III
TRANSFORMERS PARAMETERS

Transformer	Power [kVA]	Voltage ratio	Z [%]
T_G1	750	24.9 kV Y / 0.48 kV Y	1+5j
T_G2	750	4.16 kV Y / 0.48 kV Y	1+5j

TABLE IV
PROTECTION IEDS SETTINGS

Settings group	Protection IED	$I_{nominal}$ [A]	Protection functions settings			
			51 I_p [A]	51 t_{esc}	50 t_{ins} [s]	50 ESC_{ins}
Group 1: DG topology	RL1	300	375	0.030	0.100	005
	RL2	187	234	0.020	0.060	007
	RL3	187	122	0.016	0.040	008
	RL4	100	110	0.010	0.015	006
	RL5	010	017	0.005	0.010	003
Group 2: radial topology	RL1	300	360	0.010	0.090	002
	RL2	187	187	0.011	0.060	003
	RL3	187	099	0.011	0.015	005
	RL4	100	200	0.200	10.00	100
	RL5	400	800	0.200	10.00	100

A. Objective

The purpose of the evaluation of this case study is to compare the responses of a traditional protection scheme and an adaptive protection scheme to an electrical fault in the Smart Grid. The simulation technique in a single simulation environment is used to evaluate the traditional protection scheme. The proposed connectivity strategy is used to evaluate the adaptive protection scheme.

B. Test Scenarios

The case study has three test scenarios. In all scenarios, the Smart Grid was implemented in Simulink[®]. The Simulink[®] model was configured with 128 samples per cycle. The Smart Grid was simulated for 0.8 s. At 0.5 s, a three-phase fault (3F) with an impedance to the ground of 1 Ω occurred in bus 846.

1) *Scenario 1: Smart Grid without changes in topology – traditional protection scheme*

a) Description

In this scenario, the Smart Grid operated under the DG topology with EG, G1, and G2 in operation. The topology remained constant throughout the simulation. A traditional protection scheme was implemented using the configuration of the protection IEDs listed in Group 1 of Table IV. The simulation was performed in a single simulation environment to evaluate this traditional protection scheme.

b) Results

The current measured by the monitoring IEDs for each source in the Smart Grid is shown in Fig. 7. Between 0 s and 0.5 s the Smart Grid operated with the DG topology (Group 1), where EG, G1, and G2 supplied the power. The fault occurred at 0.5 s, and the RMS current of EG and G1 increased to 390 A until the fault was cleared. At the same time, the RMS current of G2 increased to 17 A. The RL4 IED tripped at 74 ms after the fault occurred at 0.5 s. Therefore, G1 was disconnected at 0.574 s from the system, as can be verified in Fig. 7. However, the fault had not been cleared. RL3 tripped at 130 ms after the fault occurred and the fault was successfully cleared at 0.630 s. It can be verified from Fig. 7 that the RMS current of EG dropped at 0.63 s.

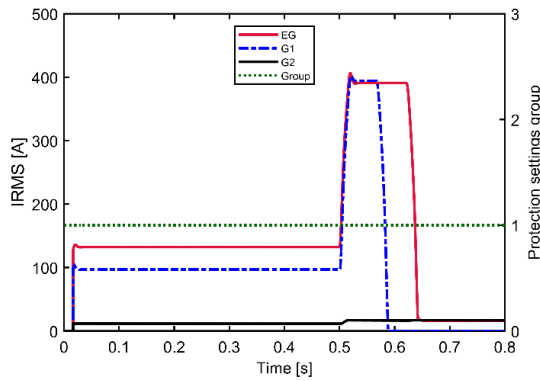


Fig. 7. The RMS of three-phase current measured by monitoring IEDs and the settings group of the protection IEDs for scenario 1.

In this scenario, the settings of protection IEDs did not change. Therefore, the protection setting group was constant at 1 throughout the simulation. The TCC curves of protection IEDs for Group 1 (Table IV) are shown in Fig. 8. At the current of 390 A at bus 846, the RL3 and RL4 will trip 130 ms and 74 ms after the fault, respectively.

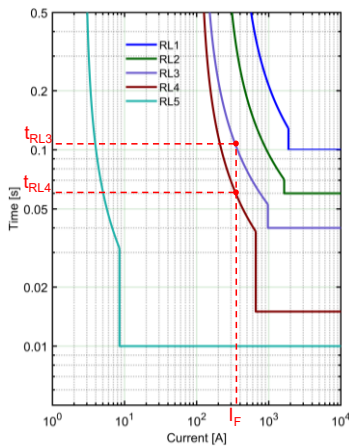


Fig. 8. TCC curves of Group 1– DG topology. Dashed red line: relays RL3 and RL4 responded to the fault current (I_f) of 390 A at bus 846.

2) Scenario 2: Smart Grid with changes in topology – traditional protection scheme

a) Description

In this scenario, the Smart Grid operated under the DG topology with both EG, G1, and G2 in operation from 0 s to 0.2 s. At 0.2 s, both the G1 and G2 were disconnected from the Smart Grid manually. The Smart Grid changed to the radial topology because only EG was in operation from 0.2 s.

The traditional protection scheme was implemented in this scenario. The parameters of the protection IEDs were static as listed in Group 1 of Table IV. The simulation was performed in a single simulation environment to evaluate this traditional protection scheme.

b) Results

The protection setting group remained constant at 1 throughout the simulation. The current measured by the monitoring IEDs for each source in the Smart Grid is shown in Fig. 9. At 0.2 s, G1 and G2 were disconnected manually and their three-phase RMS currents dropped to zero. Between 0.2 s and 0.5 s, the Smart Grid operated with the radial topology,

where only EG supplied the power. The fault occurred at 0.5 s, and the RMS current of EG increased to 390 A until the fault was cleared at 0.63 s.

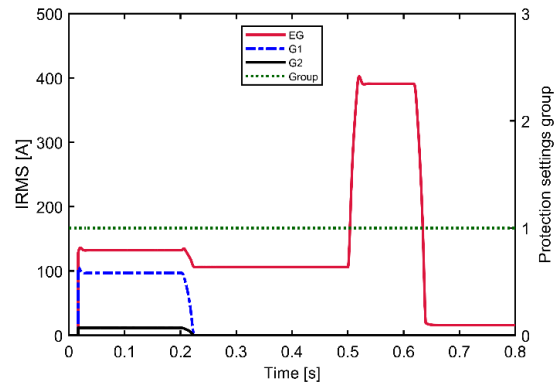


Fig. 9. The RMS of three-phase current measured by monitoring IEDs and the settings group of the protection IEDs for scenario 2.

The TCC curves of protection IEDs for Group 1 (Table IV) are shown in Fig. 10. The RL3 IED tripped at 0.63 s, after 130 ms when the fault occurred. Therefore, G1 was disconnected from the system, as can be verified in Fig. 9 at 0.63 s. In this case, RL4 and RL5 did not trip because the G1 and G2 had already been disconnected at 0.2 s before the fault occurred. This caused the open circuit and no current flowed through G1 or G2 even when the fault occurred.

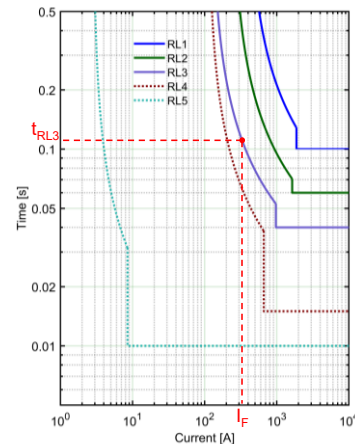


Fig. 10. TCC curves of Group 1– DG Topology. Dashed red line: response of the RL3 to the three-phase fault.

3) Scenario 3: Smart Grid with changes in topology – adaptive protection scheme

a) Description

In this scenario, the topology of the Smart Grid changed from DG to radial at 0.2 s, the same as what happened to scenario 2. From 0 s to 0.2 s, the Smart Grid operated under the DG topology with both EG, G1, and G2 in operation. From 0.2 s, only EG was in operation and the Smart Grid changed to the radial topology.

In this case, an adaptive protection scheme is used. Instead of using the fixed values, an LCC operates remotely to select and update the settings for the protection IEDs when the Smart Grid changes its topology.

The proposed connectivity strategy, which is described in Section III, is used to realize the communication between the LCC and monitoring and protection IEDs. The process of

updating the parameters of the protection IEDs is shown in Fig. 11. The transmitter-receiver block acquires the RMS currents of the sources, which are measured by the monitoring IEDs. When any of the measured RMS current changes, the transmitter-receiver block sends a message A to LCC, which contains its three-phase current RMS.

After receiving the RMS currents of all monitoring IEDs, the LCC runs its algorithm to identify the Smart Grid topology and selects the appropriate set of parameters listed in Table IV. The LCC then sends a message B to the protection IEDs, which contains the parameter settings.

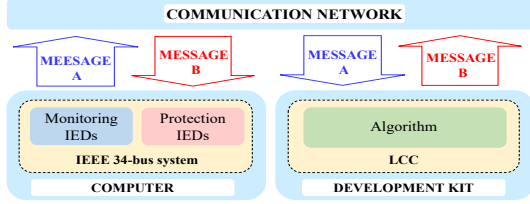


Fig. 11. Management of the protection IEDs through the LCC.

The message A is a data array that has a size of 6 bytes and has the structure shown in Fig. 12. Each monitoring IED uses 2 bytes to represent the RMS value of three-phase current—1 byte for the integer part, and the other 1 byte for the decimal part. Each of these data is of the 8-bit unsigned integer type (uint8).

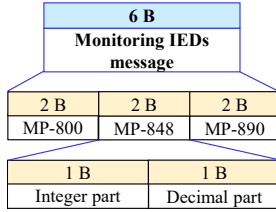


Fig. 12. Data array transmitted by the monitoring IEDs. The message A has a size of 6 bytes and each monitoring IED uses 2 bytes.

The message B is a data array that has a size of 190 bytes and has the structure shown in Fig. 13. The message B has a flag that has a size of 15 bytes. The settings for the five protection IEDs occupy a total size of 175 bytes. Each of the data is of the 8-bit unsigned integer type (uint8).

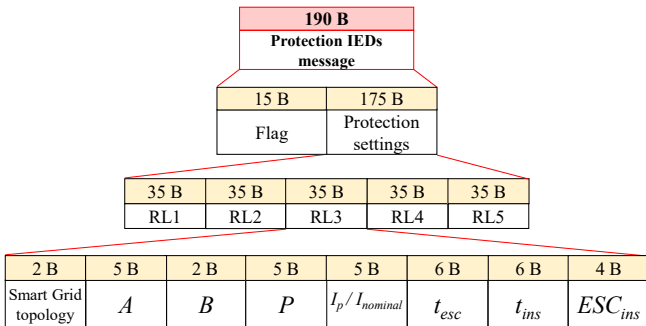


Fig. 13. Data array received by the protection IEDs. Message B has a size of 190 bytes, which is composed of a flag of 15 bytes and 175 bytes shared by 5 protection IEDs.

From the application approach described in Section III, the modified IEEE 34-bus system is implemented in Simulink®, while the LCC is implemented in the Texas Instruments®

development kit. In the development kit, the LCC algorithm is implemented as a C function. A threshold value for RMS current—1 A was selected in this paper to determine if the source is operating.

The LCC compares the selected threshold value (1 A) with the RMS of the three-phase current, which is calculated by each of the monitoring IEDs, M-P800, M-P848, and M-P890. Based on this threshold, the LCC determines the Smart Grid topology based on the conditions of Table V. Once the topology is identified, the LCC selects the parameters of the protection IEDs. The selected topology by default is DG.

TABLE V
RMS VALUES OF THE MONITORING IEDS TO IDENTIFY EACH SMART GRID TOPOLOGY

Topology	M-P800 IED	M-P848 IED	M-P890 IED
DG	Any RMS value	RMS \geq Threshold	RMS \geq Threshold
Radial	RMS \geq Threshold	RMS $<$ Threshold	RMS $<$ Threshold

The development kit and the computer are connected through a LAN in a star topology, using the Fast Ethernet standard (Fig. 14). The two end devices are connected to a layer 2 Ethernet switch. The IP router dynamically assigns IP addresses to the two terminal devices.

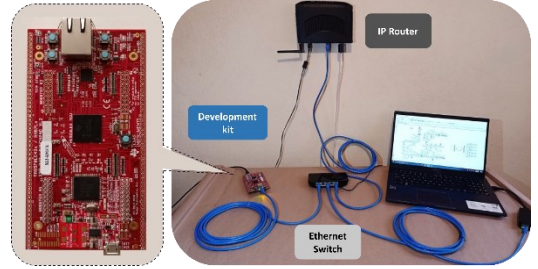


Fig. 14. The LAN implementation between the simulation environment and the embedded development kit.

The source code developed for this test scenario, in MATLAB/Simulink® and the Hercules™ RM57Lx Launchpad™ Development Kit from Texas Instruments®, is available to the reader at [40].

b) Results

In this scenario, the settings for the protection IEDs changed from Group 1 to Group 2 at 0.2 s (Fig. 15). Before 0.2 s, both G1, G2, and EG supplied power to the Smart Grid under the DG topology. At 0.2 s, G1 and G2 were disconnected manually and their three-phase RMS currents dropped to zero. Between 0.2 s and 0.5 s, the Smart Grid operated with the radial topology, where only EG supplied the power.

Before 0.2 s, the system operated as a DG topology and its TCC curves are the same as scenario 2 (Fig. 10). After 0.2 s, the setting parameters of the protection IEDs were updated and their new TCC curves are shown in Fig. 16. The fault occurred at 0.5 s, and the RMS current of EG increased to 390 A. In the new TCC curves, the RL3 IED tripped at 0.575 s, after 75 ms when the fault occurred. Therefore, the fault was cleared at 0.575 s, as can be verified in Fig. 15.

When the topology of the Smart Grid changed, the LCC received the measured RMS currents from all monitoring IEDs, identified the new topology, selected the appropriate group of setting parameters for the protection IEDs, and sent the parameters to the protection IEDs.

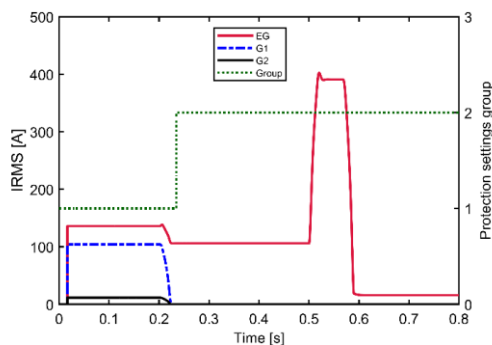


Fig. 15. The RMS of three-phase current measured by monitoring IEDs and the settings group of the protection IEDs for scenario 3.

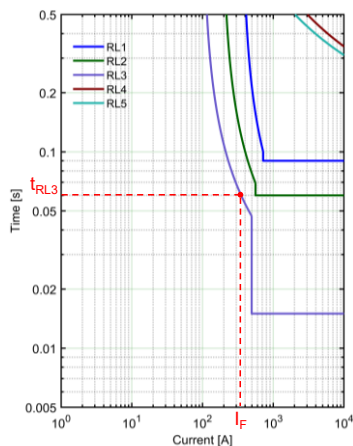


Fig. 16. TCC curves of Group 2– Radial Topology. Dashed red line: performance of relay RL3 during the fault.

The total communication delay for this process (t_{com}) is 13 ms, as can be verified in Fig. 15. This delay occurs during the updating of setting parameters for the protection IEDs.

c) Discussion

The results for the three test scenarios are summarized in Table VI. According to the results, the fault clearing speed of scenario 3, which utilized an adaptive protection scheme to change the parameters of the protection IEDs when the topology of the Smart Grid changed, was the fastest. With the adaptive protection scheme that was realized by the proposed connectivity strategy, the fault was cleared 0.055 s faster. In this paper, the proposed connectivity strategy realized the communication process in HIL. Therefore, it has enabled the measurement of the communication delay, referred to as t_{com} . Respecting the communication delay obtained in the performance evaluation in Section III, for the corresponding message sizes in the case study, the obtained value falls within the 95% confidence interval. This suggests that the communication delay obtained in the case study is consistent with the expected variability of the data.

TABLE VI
RESULTS OF THE TEST SCENARIOS

Scenario	Fault current [A]	Tripping time [ms]	Tripped IED	Message A size [B]	Message B size [B]	t_{com} [ms]
1	390	74, 130	RL4, RL3	None	None	None
2	390	130	RL3	None	None	None
3	390	75	RL3	6	190	13

V. CONCLUSION

The proposed connectivity strategy, implemented in Hardware-in-the-loop, facilitates real-time data transmission among different components in a Smart Grid via a local area network (LAN). It enables the measurement of communication delay and provides a low-cost testing platform for evaluating new Smart Grid functionalities.

A Smart Grid model with some of its components implemented in simulation environments (MATLAB/Simulink[®]) and other components in embedded systems (Texas Instruments[®] development kit) was used to validate the proposed connectivity strategy. When the topology of the Smart Grid changed, the proposed connectivity strategy detected the changes and updated the parameter settings of the protection devices in 13 ms. As a result, the Smart Grid cleared the fault 0.055 s faster.

FUTURE WORK

In this work, the Smart Grid components have focused on the application of distribution system automation. Therefore, as future work, it is proposed to expand the scope of the connectivity strategy for its use in other Smart Grid functionalities. Furthermore, we propose to scale the proposal to enable the connection of additional end devices and assess the performance of distributed simulation.

REFERENCES

- [1] C. Greer *et al.*, “NIST Framework and Roadmap for Smart Grid Interoperability Standards, Release 3.0,” Gaithersburg, MD, Oct. 2014. doi: 10.6028/NIST.SP.1108r3.
- [2] M. A. Judge, A. Khan, A. Manzoor, and H. A. Khattak, “Overview of smart grid implementation: Frameworks, impact, performance and challenges,” *J. Energy Storage*, vol. 49, no. August 2021, p. 104056, 2022, doi: 10.1016/j.est.2022.104056.
- [3] K. C. Budka, J. G. Deshpande, T. L. Doumi, M. Madden, and T. Mew, “Communication network architecture and design principles for smart grids,” *Bell Labs Tech. J.*, vol. 15, no. 2, pp. 205–227, Aug. 2010, doi: 10.1002/bltj.20450.
- [4] M. Ghorbanian, S. H. Dolatabadi, M. Masjedi, and P. Siano, “Communication in smart grids: A comprehensive review on the existing and future communication and information infrastructures,” *IEEE Syst. J.*, vol. 13, no. 4, pp. 4001–4014, 2019, doi: 10.1109/JSYST.2019.2928090.
- [5] G. Dileep, “A survey on smart grid technologies and applications,” *Renew. Energy*, vol. 146, pp. 2589–2625, 2020, doi: 10.1016/j.renene.2019.08.092.
- [6] E. Ancillotti, R. Bruno, and M. Conti, “The role of communication systems in smart grids: Architectures, technical solutions and research challenges,” *Comput. Commun.*, vol. 36, no. 17–18, pp. 1665–1697, Nov. 2013, doi: 10.1016/j.comcom.2013.09.004.

- [7] T. Strasser, M. Stifter, F. Andren, and P. Palensky, "Co-Simulation Training Platform for Smart Grids," *IEEE Trans. Power Syst.*, vol. 29, no. 4, pp. 1989–1997, Jul. 2014, doi: 10.1109/TPWRS.2014.2305740.
- [8] G. A. Sigurdsson and M. F. Abdel-Fattah, "Smart Grids Simulation Tools: Overview and Recommendations," in *2021 IEEE 62nd International Scientific Conference on Power and Electrical Engineering of Riga Technical University (RTUCON)*, Nov. 2021, pp. 1–6, doi: 10.1109/RTUCON53541.2021.9711583.
- [9] M. Ali, M. Zakariya, M. Asif, and A. Ullah, "TCP/IP Based Intelligent Load Management System in Micro-Grids Network Using MATLAB/Simulink," *Energy Power Eng.*, vol. 04, no. 04, pp. 283–289, 2012, doi: 10.4236/epe.2012.44038.
- [10] Z. CAI and M. YU, "Modeling and Simulation of a Real-time Ethernet Protocol for Smart Grids," *Int. J. Intell. Control Syst.*, vol. 17, no. 3, pp. 69–78, 2012.
- [11] W. Li, M. Ferdowsi, M. Stevic, A. Monti, and F. Ponci, "Cosimulation for Smart Grid Communications," *IEEE Trans. Ind. Informatics*, vol. 10, no. 4, pp. 2374–2384, Nov. 2014, doi: 10.1109/TII.2014.2338740.
- [12] M. Garau, G. Celli, E. Ghiani, F. Pilo, and S. Corti, "Evaluation of Smart Grid Communication Technologies with a Co-Simulation Platform," *IEEE Wirel. Commun.*, vol. 24, no. 2, pp. 42–49, Apr. 2017, doi: 10.1109/MWC.2017.1600214.
- [13] M. A. E. Elabbas, A. M. E. Awad, and S. F. Babikir, "Agent based load management for Microgrid," in *2017 International Conference on Communication, Control, Computing and Electronics Engineering (ICCCCEE)*, Jan. 2017, pp. 1–6, doi: 10.1109/ICCCCEE.2017.7867684.
- [14] F. Guo *et al.*, "Design and development of a reconfigurable hybrid Microgrid testbed," in *2013 IEEE Energy Conversion Congress and Exposition*, Sep. 2013, pp. 1350–1356, doi: 10.1109/ECCE.2013.6646862.
- [15] D. Celeita, M. Hernandez, G. Ramos, N. Penafiel, M. Rangel, and J. D. Bernal, "Implementation of an educational real-time platform for relaying automation on smart grids," *Electr. Power Syst. Res.*, vol. 130, pp. 156–166, Jan. 2016, doi: 10.1016/j.epsr.2015.09.003.
- [16] V. A. Papaspiliotopoulos, G. N. Korres, V. A. Kleftakis, and N. D. Hatzigiorgiou, "Hardware-In-the-Loop Design and Optimal Setting of Adaptive Protection Schemes for Distribution Systems With Distributed Generation," *IEEE Trans. Power Deliv.*, vol. 32, no. 1, pp. 393–400, Feb. 2017, doi: 10.1109/TPWRD.2015.2509784.
- [17] H. Palahalli, E. Ragaini, and G. Gruosso, "Smart Grid Simulation Including Communication Network: A Hardware in the Loop Approach," *IEEE Access*, vol. 7, pp. 90171–90179, 2019, doi: 10.1109/ACCESS.2019.2927821.
- [18] A. I. Narvaez-Villota, A. J. Ustariz-Farfan, L. F. Diaz-Cadavid, J. A. Ocampo-Wilches, and E. A. Cano-Plata, "Development of a Methodology for Data Flow over TCP/IP for a Protection Scheme in Smart Grids," *2019 IEEE Work. Power Electron. Power Qual. Appl. PEPQA 2019 - Proc.*, 2019, doi: 10.1109/PEPQA.2019.8851536.
- [19] UPME, "Smart Grids Colombia VISIÓN 2030. Parte 1 - Antecedentes y Marco Conceptual del Análisis, Evaluación y Recomendaciones para la Implementación de Redes Inteligentes en Colombia." 2016, [Online]. Available: http://www.upme.gov.co/DemandayEficiencia/Doc_Hemeroteca/Smart_Grids_Colombia_Vision_2030/1_Parte1_Proyecto_BID_Smart_Grids.pdf.
- [20] B. K. Duncan and B. G. Bailey, "Protection, Metering, Monitoring, and Control of Medium-Voltage Power Systems," *IEEE Trans. Ind. Appl.*, vol. 40, no. 1, pp. 33–40, Jan. 2004, doi: 10.1109/TIA.2003.821809.
- [21] F. Buchholz, "Das Begriffssystem Rechtleistung. Wirkleistung, totale Blindleistung," 1950.
- [22] J. A. Ocampo Wilches, "ANÁLISIS EN MICRORREDES: Estrategias de Coordinación de Protecciones Inteligentes," p. 110, 2019, [Online]. Available: <https://repositorio.unal.edu.co/handle/unal/76108>.
- [23] "IEEE Standard for Inverse-Time Characteristics Equations for Overcurrent Relays," *IEEE Std C37.112-2018 (Revision of IEEE Std C37.112-1996)*, pp. 1–25, 2019, doi: 10.1109/IEEESTD.2019.8635630.
- [24] T. S. Ustun, C. Ozansoy, and A. Zayegh, "Modeling of a centralized microgrid protection system and distributed energy resources according to IEC 61850-7-420," *IEEE Trans. Power Syst.*, vol. 27, no. 3, pp. 1560–1567, 2012, doi: 10.1109/TPWRS.2012.2185072.
- [25] T. S. Ustun, R. H. Khan, A. Hadbah, and A. Kalam, "An adaptive microgrid protection scheme based on a wide-area smart grid communications network," *2013 IEEE Latin-America Conf. Commun. LATINCOM 2013 - Conf. Proc.*, 2013, doi: 10.1109/LatinCom.2013.6759822.
- [26] J. A. Ocampo-Wilches, A. J. Ustariz-Farfan, and E. A. Cano-Plata, "Modeling of a centralized microgrid protection scheme," *2017 3rd IEEE Work. Power Electron. Power Qual. Appl. PEPQA 2017 - Proc.*, 2017, doi: 10.1109/PEPQA.2017.7981652.
- [27] E. Planas, J. Andreu, J. I. Gárate, I. Martínez de Alegría, and E. Ibarra, "AC and DC technology in microgrids: A review," *Renew. Sustain. Energy Rev.*, vol. 43, pp. 726–749, 2015, doi: 10.1016/j.rser.2014.11.067.
- [28] L. F. F. de Almeida *et al.*, "Control networks and smart grid teleprotection: Key aspects, technologies, protocols, and case-studies," *IEEE Access*, vol. 8, pp. 174049–174079, 2020, doi: 10.1109/ACCESS.2020.3025235.
- [29] J. F. Kurose and K. W. Rose, *Computer Networking: A Top-Down Approach*, 6th ed. 2013.
- [30] "Dynamic Host Configuration Protocol, RFC 2131." 1997, [Online]. Available: <https://tools.ietf.org/html/rfc2131>.
- [31] *IEEE Std 802.3u-1995 -IEEE Standards for Local and Metropolitan Area Networks*. 1995.
- [32] *1646-2004 - IEEE Standard Communication Delivery Time Performance Requirements for Electric Power Substation Automation*. IEEE, 2005.
- [33] Texas Instruments, "RM57L843 Hercules™ Microcontroller Based on the ARM® Cortex® -R Core," 2016. [Online]. Available: <https://www.ti.com/lit/ds/symlink/rm57l843.pdf>.
- [34] The MathWorks Inc, "Instrument Control Toolbox™ User's Guide ©." 2019.
- [35] S. Goldschmidt and D. Ziegelmeier, "lwIP - A Lightweight TCP/IP stack - Sumario." <http://savannah.nongnu.org/projects/lwip/> (accessed Mar. 01, 2023).
- [36] A. Dunkels, "Design and Implementation of the lwIP TCP/IP Stack." Swedish Institute of Computer Science, 2001.
- [37] E. Ding, "HALCoGen Ethernet Driver With lwIP Integration Demo and Active Web Server Demo," 2019. <https://www.ti.com/lit/an/spna239/spna239.pdf> (accessed Mar. 01, 2023).

- [38] W. H. Kersting, "Radial distribution test feeders," in *2001 IEEE Power Engineering Society Winter Meeting. Conference Proceedings (Cat. No.01CH37194)*, 2001, vol. 2, no. WINTER MEETING, pp. 908–912, doi: 10.1109/PESW.2001.916993.
- [39] R. C. Dugan and W. H. Kersting, "Induction machine test case for the 34-bus test feeder -description," in *2006 IEEE Power Engineering Society General Meeting*, 2006, p. 4 pp., doi: 10.1109/PES.2006.1709506.
- [40] GICEP, GREDYP, and GTT, "Smart Grids Repository," 2023.
https://github.com/REPOSGICEPGREDYPGTT/COMUNICACIONES_SG_PAPER.



Ana Isabel Narváez Villota was born in Pasto, Colombia in 1994. She received the Bachelor's degrees in Electronic Engineering in 2017 and Electrical Engineering in 2018, and a Master's degree in Electrical Engineering in 2021 from the Universidad Nacional de Colombia, Manizales Campus. Her research interests include Smart Grids,

Communications Networks, and Protection Coordination.



Armando J. Ustariz Farfán was born in Urumita (Colombia) in 1973. He received a bachelor's degree in Electrical Engineer in 1997, and a Master's in Electric Power in 2000 from the Universidad Industrial de Santander. He received the Ph.D. degree in Electrical Engineering at the Universidad Nacional de Colombia, in 2011. He is a researcher and associated professor with

the Electrical, Electronic and Computer Engineering Department, at Universidad Nacional de Colombia, Manizales Branch. His research interests include Power Definitions Under Non-Sinusoidal Conditions, Smart Grids, Power Quality, and Power Electronic. He is the current director of the Power Quality and Power Electronics Research Group – GICEP.



Luis Fernando Díaz Cadavid, is a Telecommunications Engineer with a Master of Science in Telecommunications Engineering degree from The Bonch-Bruevich Saint-Petersburg State University of Telecommunications-Russia, specialized in "Computing and Computation" at the University of

Cantabria – Spain. He received the Doctorate degree in Engineering in 2015 from Universidad Nacional de Colombia. He is a researcher and associated professor with the Electrical, Electronic and Computer Engineering Department, at Universidad Nacional de Colombia, Manizales Branch. His research interests include Electromagnetic compatibility and Telecommunications networks. He is the current director of

the Telematics and Telecommunications Research Group – GTT.